MUTATION IN BRIEF

HUMAN MUTATION

Mutations in the *GUCA1A* Gene Involved in Hereditary Cone Dystrophies Impair Calcium-mediated Regulation of Guanylate Cyclase

Veronique B.D. Kitiratschky[1], Petra Behnen[2], Ulrich Kellner[3], John R Heckenlively[4], Eberhart Zrenner[5], Herbert Jägle[5], Susanne Kohl[1], Bernd Wissinger[1], and Karl-Wilhelm Koch[2]

[1]Molecular Genetics Laboratory, Institute for Ophthalmic Research, Centre for Ophthalmology, University Tübingen, Tübingen, Germany; [2]Institute of Biology and Environmental Sciences, Biochemistry group, University of Oldenburg, Oldenburg, Germany; [3]RetinaScience, Bonn, Germany; [4] University of Michigan, Kellogg Eye Center University of Michigan, Kellogg Eye Center, [5]Centre for Ophthalmology, University Tübingen, Tübingen, Germany

*Correspondence to Karl-Wilhelm Koch, Institute of Biology and Environmental Sciences, Biochemistry group, University of Oldenburg; tel: +49-441-798-3640; E-mail: karl.w.koch@uni-oldenburg.de

Contract grant sponsor: German Research Council, EU, ProRetina; Contract grant number: KFO134 - Ko2176/1, LSHG-CT-2005-512036, Pro-Re/Prom-Stip.Koch/Behnen

Communicated by Daniel F. Schorderet

ABSTRACT: The *GUCA1A* gene encodes the guanylate cyclase activating protein 1 (GCAP1) of mammalian rod and cone photoreceptor cells, which is involved in the Ca^{2+}-dependent negative feedback regulation of membrane bound guanylate cyclases in the retina. Mutations in the *GUCA1A* gene have been associated with different forms of cone dystrophies leading to impaired cone vision and retinal degeneration. Here we report the identification of three novel and one previously detected *GUCA1A* mutations: c.265G>A (p.Glu89Lys), c.300T>A (p.Asp100Glu), c.476G>T (p.Gly159Val) and c.451C>T (p.Leu151Phe). The clinical data of the patients carrying these mutations were compared with the functional consequences of the mutant GCAP1 forms. For this purpose we purified the heterologously expressed GCAP1 forms and investigated whether the mutations affected the Ca^{2+}-triggered conformational changes and the apparent interaction affinity with the membrane bound guanylate cyclase. Furthermore, we analyzed Ca^{2+}-dependent regulatory modes of wildtype and mutant GCAP1 forms. Although all novel mutants were able to act as a Ca^{2+}-sensor protein, they differed in their Ca^{2+}-dependent activation profiles leading to a persistent stimulation of guanylate cyclase activities at physiological intracellular Ca^{2+} concentration. © 2009 Wiley-Liss, Inc.

KEY WORDS: *GUCA1A*, GCAP1, guanylate cyclase activator, biochemical analysis, genotype-phenotype correlation

INTRODUCTION

Inherited progressive cone rod dystrophies (CRD) are characterized by progressive loss of cone photoreceptor function followed by progressive loss of rod photoreceptor function and are often accompanied by retinal degeneration (Hamel, 2007; Merin, 2005; Michaelides, et al., 2006). In contrast, in inherited progressive cone

Received 3 December 2008; accepted revised manuscript 22 April 2009.

DOI: 10.1002/humu.21055

dystrophies (CD) only cone function is impaired and retinal degeneration is often minimal and confined to the central retina. All modes of Mendelian inheritance have been observed and genetic heterogeneity is a hallmark of both CD and CRD (Hamel, 2007).

Heterozygous mutations in the *GUCA1A* gene (MIM# 600364) have been identified to cause autosomal dominantly inherited CD, CRD, and macular dystrophy (adCD, adCRD, adMD) (Downes, et al., 2001; Jiang, et al., 2005; Michaelides, et al., 2005; Nishiguchi, et al., 2004; Payne, et al., 1998; Sokal, et al., 2005; Wilkie, et al., 2001).

The *GUCA1A* gene encodes one of three human guanylate cyclase activating proteins, GCAP1, which is expressed in rod and cones in the human retina, with stronger GCAP1 immunoreactivity in cones than in rods (Cuenca, et al., 1998). Excitation of the photoreceptor decreases the intracellular concentration of cyclic guanosine-3´, 5´- monophosphate (cGMP) and Ca^{2+}. GCAP1 works as a Ca^{2+}-sensor protein that detects changes in Ca^{2+} concentration and stimulates membrane bound guanylate cyclases in a Ca^{2+}-dependent manner. By this step the cGMP pool of the photoreceptor is replenished (Palczewski et al., 1994; Frins et al., 1996; Haeseleer, et al., 1999). Electrophysiological analyses in retinal explants and living mice showed that deletion of GCAP1 and GCAP2 delay the recovery of light responses in rods and cones. Notably, GCAP1 restores recovery of rod and cone responses in the absence of GCAP2. GCAP1 is thus important to regain the dark-adapted state after excitation of the photoreceptor (Mendez, et al., 2001; Pennesi, et al., 2003).

So far, only seven putative pathogenic mutations in the GUCA1A gene have been reported in patients with adCD, adCRD or adMD: p.Pro50Leu, p.Tyr99Cys, p.Asn104Lys, p.Thr114Ile, p.Ile143delinsAsnThr, p.Leu151Phe, and p.Glu155Gly (Dizhoor, et al., 1998; Downes, et al., 2001; Jiang, et al., 2005; Michaelides, et al., 2005; Nishiguchi, et al., 2004; Payne, et al., 1998; Sokal, et al., 2005; Wilkie, et al., 2001 Jiang et al., 2008). Here we report the identification of three novel and one previously published *GUCA1A* gene mutations in patients with adCD and adCRD. We present clinical data and a detailed functional and molecular characterization of the mutant proteins with a focus on their Ca^{2+}-sensing and guanylate cyclase regulating properties. For this purpose, we constructed the corresponding mutants, purified the heterologously expressed proteins and employed the purified GCAP1 forms in the analyses.

METHODS

Subjects and diagnostic criteria

Patients diagnosed with CD or CRD according to standard diagnostic criteria (Merin, 2005) and a family history consistent with an autosomal dominant mode of inheritance were included in the study and recruited in the Centre for Ophthalmology, Tübingen, Germany and ophthalmic specialist centers throughout Europe and the United States of America. The diagnosis of adCD or adCRD was mainly based on the results of full field electroretinography (ERG), performed according to ISCEV standard (Marmor, et al., 2004). Patients with reduced cone ERGs and normal rod ERGs were diagnosed as adCD, whereas patients with reduced cone and rod ERGs were diagnosed as adCRD. Characteristic symptoms, fundus and visual field results were used to corroborate the diagnosis. The study was performed according to the tenets of the Declaration of Helsinki and approved by the ethical committees of the participating institutions. Informed consent was obtained from all patients.

Mutation analysis and exclusion of novel sequence variants in normal controls

Mutation analysis of all four coding exons of the *GUCA1A* gene was performed by direct DNA sequencing of polymerase chain reaction (PCR) amplified genomic DNA using four sets of gene specific primer pairs (primers available upon request). PCR products were enzymatically purified applying ExoSap-IT reagent (USB, Cleveland, OH, USA) and subsequently sequenced using BigDye Sequencing Chemistry (Applied Biosystems, Darmstadt, Germany). Sequencing products were separated on a 3100 capillary sequencer (Applied Biosystems) and sequences scanned for mutations by computer-assisted manual inspection. We used GUCA1A mRNA sequence NM_000409.2 and the corresponding consensus coding sequence CCDS4864.1 as references. Nucleotide numbering reflects cDNA numbering with +1 corresponding to the A of the ATG translation initiation codon in the

reference sequence, according to journal guidelines (www.hgvs.org/mutnomen). The initiation codon is codon 1. Sequence variant descriptions were checked using the Mutalyzer program (Wildeman, et al., 2008).

Novel sequence variants were excluded in 200 chromosomes by means of PCR and subsequent restriction length polymorphism analysis (PCR/RFLP) with the following restriction enzymes: HphI for c.265G>A (enzyme recognition site 5´-3´ GGTG**A**, position of mutated nucleotide bold), BsaBI for c.300T>A (GA**T**NNNNATC) and, BsaHI for c.476G>T (G**A/G**CGC/TC). Restriction enzymes were supplied by New England Biolabs, Beverly, MA, USA. To detect the sequence variant c.300T>A a recognition site was introduced with mismatch primer 5´-ggtacttcaagctctacgaAgtggacggcaacg-3´ (mismatched nucleotide capital letter, c.300T nucleotide directly 3´ to mismatch primer) paired with exon 4 forward primer. PCR products were digested overnight and the RFLP pattern was evaluated by agarose gel electrophoresis.

Alignment of human GCAP1 and orthologous proteins

Human and orthologous GCAP1 protein sequences were derived from the UniProt database (http://www.expasy.uniprot.org/, UniProt database accession numbers P46065, P79880, P43080, P43081, Q8QFN1, Q90WX4) and a global multiple alignment was performed using the Clustal W algorithm (Thompson, et al., 1994).

Generation of mutant GCAP1 expression vectors

The novel sequence variants c.265G>A (p.Glu89Lys), c.300T>A (p.Asp100Glu), and c.476G>T (p.Gly159Val) were introduced into the vectors pET21-bGCAP1 and pET21-bGCAP1-D6S (Hwang and Koch, 2002a) by site-directed in vitro mutagenesis using the QuikChange Site-Directed Mutagenesis Kit according to the manufacturer´s protocol (Stratagene, La Jolla, CA, USA) (primers available upon request). Mutagenized constructs were sequenced to confirm the presence of desired mutations and the absence of undesired second-site mutations.

Heterologous expression and purification of GCAP1

Wildtype and mutant GCAP1 forms were obtained by overexpression in BL21 *E.coli* cells and purified by a combination of ammoniumsulfate precipitation, SEC and ion exchange chromatography on a UnoQ-column (BioRad Life Science Group, Hercules, CA) as described before (Hwang and Koch, 2002; Koch and Helten, 2008). In all assays with purified proteins the myristoylated form of GCAP1 was used. Myristoylation was verified by reversed phase high performance liquid chromatography analysis (Hwang and Koch, 2002b).

Tryptophane (Trp) fluorescence spectroscopy

Intrinsic Trp fluorescence measurements were performed with a spectrometer from Photon Technology International (Birmingham, New Jersey, USA) as described before (Koch and Helten, 2008). Lyophilized samples of GCAP1 forms were dissolved in bidistilled water containing 1 mM DTT and a concentration of 70-120 µM. The protein stock was diluted in fluorescence buffer (80 mM Hepes pH 7.5, 40 mM KCl, 1 mM DTT) at a final concentration of 0.7-1.2 µM. Measurements were also performed in the presence 1 mM of $MgCl_2$. The excitation wavelength was set to 280 nm, the emission spectrum was recorded from 300-420 nm. Different free Ca^{2+} concentrations were adjusted by a set of Ca^{2+}/EGTA buffer solution (Hwang et al., 2003).

Guanylate cyclase assay

Guanylate cyclase (GC) activity in the presence of recombinant GCAP1 forms was determined by using washed bovine rod outer (ROS) segment membranes that mainly contain ROS-GC1 (encoded by the GUCY2D gene) but are, due to the washing process, devoid of intrinsic GCAP activity (Helten et al., 2007). GC activities were measured according to a recently published detailed protocol (Koch and Helten, 2008) by reconstituting washed ROS membranes that are devoid of intrinsic GCAP activity with myristoylated, recombinant GCAP1 forms.

Protein Electrophoresis and gel shift assay

Standard biochemical techniques as sodium dodecylsulfate polyacrylamide gel electrophoresis (SDS-PAGE) and the determination of protein concentrations were done according to established protocols (Laemmli, 1970; Bradford, 1976). Gel shift assays were performed as previously published (Hwang and Koch, 2002a). They display Ca^{2+}-induced changes in electrophoretic mobility and serve as a qualitative test for Ca^{2+}-induced conformational changes under denaturating conditions.

RESULTS

Mutation analysis of the *GUCA1A* gene in patients with adCD and adCRD

24 unrelated patients met the clinical inclusion criteria and were included in the study. 19 patients had adCD and five patients had adCRD. All patients were screened for mutations in all coding exons of the *GUCA1A* gene. Thereby, mutations in four of 24 unrelated patients were discovered: the known mutation c.451C>T (p.Leu151Phe) (Jiang, et al., 2005) in patient ZD1/1737 (pedigree identifier III:8) , and three novel nucleotide substitutions: c.265G>A (p.Glu89Lys) in patient ZD182/12121 (II:2), c.300T>A (p.Asp100Glu) in patient ZD191/12956 (III:2), and c.476G>T (p.Gly159Val) in patient ZD172/11798 (II:1) (Fig. 1). None of the novel mutations were found by PCR/RFLP analysis in a screen of 200 chromosomes from normal controls.

A global multiple sequence alignment including human, bovine and murine sequences as well as sequences of chicken, D. rerio and F. rupiens showed that all mutations affected amino acid residues that are highly conserved among different species. Moreover, all mutations were located in functionally important domains: p.Glu89Lys and p.Gly159Val are located in the flanking helices of the Ca^{2+}-binding EF-hand 3 and 4, while p.Asp100Glu and p.Leu151Phe are situated in the Ca^{2+}-binding loops.

Segregation of the mutant allele with the disease phenotype was demonstrated in families ZD1, ZD191, and ZD172 (Fig. 1). In family ZD182 the brother of the index patient is a mutation carrier too but his clinical status is unknown. The mother suffers from toxic retinopathy after longstanding therapeutic chloroquine intake and is not a mutation carrier. The clinical status of the father is unknown and his DNA was unavailable for segregation analysis.

Phenotype of patients with *GUCA1A* gene mutations

Detailed clinical data were available for seven patients with *GUCA1A* mutations. Six of seven patients presented with adCD and one patient had adCRD. Two patients with CD had a differential diagnosis of macular dystrophy and mild maculopathy, respectively. Another patient had adCD and glaucoma. Disease onset was between 15 years and 26 years of age (Table 1). Four patients had poor visual acuity (VA) below 0.1 (median age at examination 61 years). Two patients had good or fairly good visual acuity for both eyes (ZD1/2093/F, age 18, disease duration 3 years: VA 1.0/1.0; ZD182/12121/M, age 33, disease duration 13 years: VA 0.4/0.5), and one patient had fairly good visual acuity in one eye (ZD191/15859/F, age 60, disease not documented: VA HM/0.5). Glare sensitivity and color vision was typically abnormal and one of the first symptoms, whereas night vision was normal. Fundus changes were confined to the macula, ranging from fine granular retinal pigment epithelium defects to large regions of atrophy in the retinal pigment epithelium and choriocapillaris. The outer borders of the visual field were normal in all patients with adCD, but was narrowed in the patient with adCRD. All patients with long standing disease and for whom information was available also had central scotoma. Scotopic and photopic ERG was below detection limit in one patient (ZD172/16033/M) who suffered from the disease for over 60 years. However, most patients, even those with longstanding disease still had normal or almost normal Ganzfeld-ERGs.

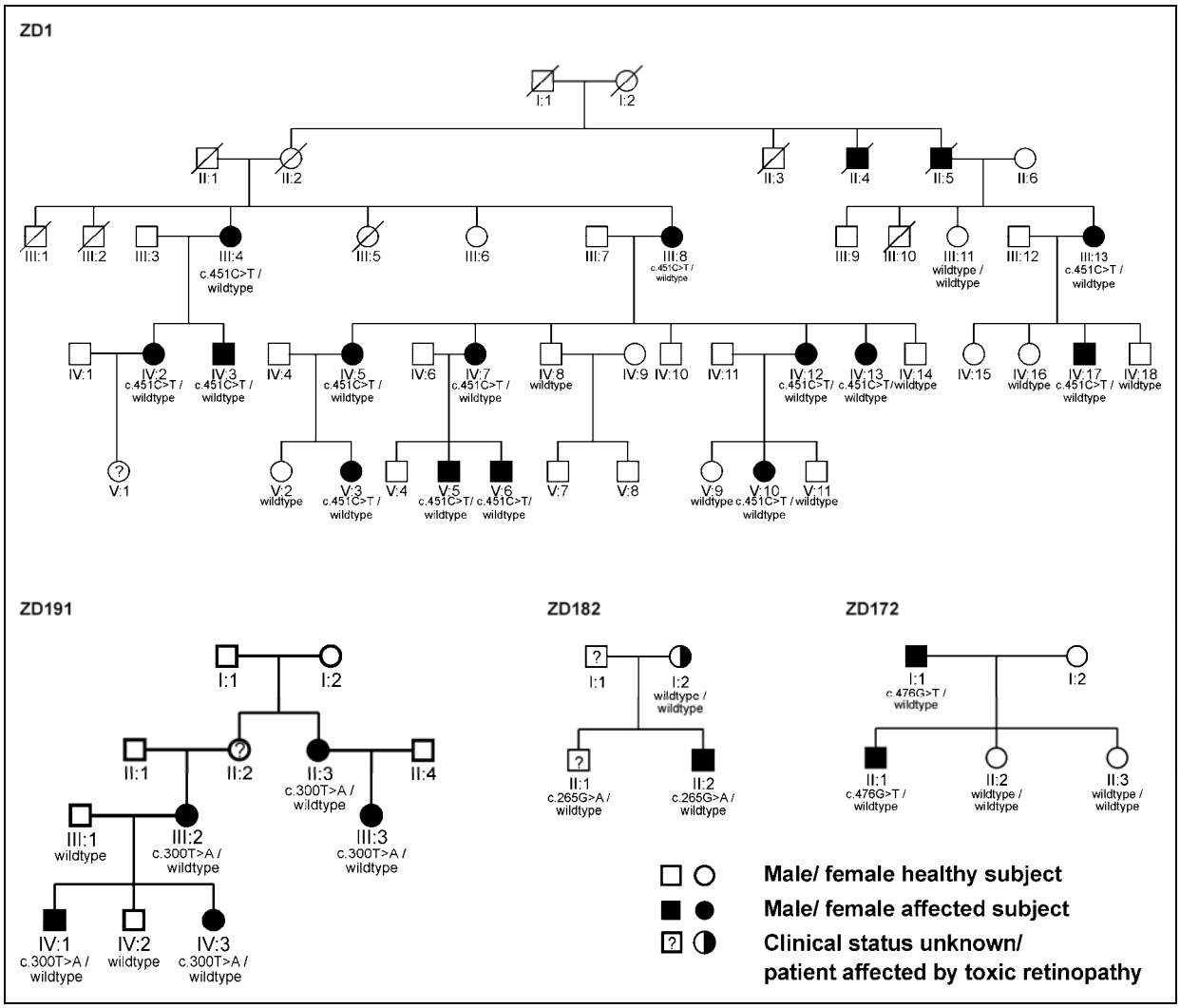

Figure 1. Segregation of the mutant allele with the disease phenotype demonstrated in families ZD 1, ZD 191, and ZD 172. In family ZD 182 segregation could not be fully elucidated due to unavailability of the father´s DNA.

Table 1. Phenotype and electrophysiological data of index patients and relatives with *GUCA1A* gene mutations.

Family ID/ Patient ID/ Gender	Mutation	Diagnosis	Age of onset	Age at examination	BCVA (OD/OS)	Color vision[1]	Glare sensitivity	Night vision	RPE atrophy/ Choroidal atrophy/ RPE clumping				Additional fundus findings[1]	Visual Field[1]		Scotopic GF-ERG [1, 2]				Photopic GF-ERG [1, 2]				mfERG[1]
																rod response		mixed rod cone response		single flash		30 Hz flicker		
																A	I	A	I	A	I	A	I	
ZD182/12121/M	c.265G>A p.E89K	CD or macular dystrophy	20	33	0.4/0.5	PD15 sat: scotopic defect	increased	normal	M				mild macular pigment changes	C	reduced sensitivity	N	N	N	N	N	Pro-longed	N	N	central and ring 2 + 3 reduced amplitude, normal implicit time
									P					P	N									
ZD191/15859/F	c.300T>A p.D100E	CD and glaucoma	n.i.	60	HM/0.5	n.i.	n.i.	n.i.	M	n.i.	n.i.	n.i.		C	n.i.	N	N	n.i.	n.i.	bN	bN	bN	bN	n.i.
									P	n.i.	n.i.	n.i.		P	n.i.									
ZD1/2093/F	c.451C>T p.L151F*	CD or mild maculopathy	15	18	1.0/1.0	PD15 sat: tritan defect, anomalo-scope: protano-maly	increased	normal	M				normal fundus	C	N	N	N	N	N	N	Pro-longed	N	N	n.i.
									P					P	N									
ZD1/2081/F	c.451C>T p.L151F*	CD	20	41	0.05/0.1	PD15 sat: protan and tritan defect, anomalo-scope: protano-maly	increased	normal	M	**X**			fine granular retinal pigment atrophy	C	central scotoma	N	N	N	N	N	Pro-longed	n.i.	n.i.	n.i.
									P					P	N									

Table 1. Phenotype and electrophysiological data of index patients and relatives with *GUCA1A* gene mutations.

Family ID/ Patient ID/ Gender	Mutation	Diagnosis	Age of onset	Age at examination	BCVA (OD/OS)	Color vision[1]	Glare sensitivity	Night vision	RPE atrophy/ Choroidal atrophy/ RPE clumping			Additional fundus findings[1]	Visual Field[1]		Scotopic GF-ERG [1, 2]				Photopic GF-ERG [1, 2]				mfERG[1]
															rod response		mixed rod cone response		single flash		30 Hz flicker		
															A	I	A	I	A	I	A	I	
ZD1/1737/F	c.451C>T p.L151F*	CD	25	67	0.05/0.1	PD15 sat: protan/ deutan defect	increased	normal	M	**X**	**X**	central geographic atrophy, periphery normal	C	central scotoma	bN	bN	n.i.	n.i.	↓↓	Pro-longed	n.i.	n.i.	n.i.
									P				P	N									
ZD172/11798 /M	c.476G>T p.G159V	CD	26	55	0.05/0.05	PD15 desat: no colour differences detected	increased	normal	M	**X**	**X**	central geographic atrophy, periphery normal, pale temporal optic disc, bilateral	C	central scotoma	N	N	bN	N	reduced	Pro-longed	reduced	prolonged	central ring no responses, ring 2-3 severely reduced, ring 4-5 moderately reduced responses, delayed implicit time
									P				P	N									
ZD172/16033 /M	c.476G>T p.G159V	CRD	20	81	0.05/HM	n. i.	increased	n.i.	M	**X**	**X**	central geographic atrophy, peripheral few bone spicules, bilateral	C	central scotoma prior to narrowing of peripheral visual field	ext.	ext.	reduced	Pro-longed	ext.	ext.	ext.	ext.	n. i.
									P		**X**		P										

ID, identification number; BCVA, best corrected Snellen visual acuity; OD, right eye; OS, left eye; RPE, retinal pigment epithelium; GF-ERG, full field electroretinography; A, amplitude; I, implicit time; HM, perceiving hand movements; PD15, Panel D15 Color vision test; sat, saturated; desat, desaturated; n.i., no information; PD, papilla diameter; M, Macula; P, Periphery; C, Central visual field; N, normal; bN, borderline normal data within normal range but near the 5th quantile of normal values; ext., extinct or below detection limit; reduced/prolonged, value outside normal range; [1] both eyes are identical for all features unless stated; [2] normal range 5-95% confidence interval of normal values, * mutation previously reported by Jiang, L. et al. 2005

Functional analyses

All three novel mutations affect highly conserved amino acid residues in the functionally critical Ca^{2+}-binding domains EF-hand 3 and 4 (as reviewed but not shown) prompting us to investigate the functional implications of these mutations. In particular we asked whether the mutations impair Ca^{2+}-triggered conformational changes and modify or disable the Ca^{2+}-dependent regulation of guanylate cyclase activities. For these purposes we heterologously expressed wildtype and mutant forms of GCAP1 in E. coli, purified the proteins to apparent homogeneity and analyzed their functional properties.

Ca^{2+}-induced conformational changes as assayed with Ca^{2+}-gel shift assay and Tryptophane fluorescence

Ca^{2+}-gel shift assay.

As a qualitative test for Ca^{2+}-induced conformational changes we used a Ca^{2+}-gel shift assay: GCAPs like other Ca^{2+}-binding proteins display different electrophoretic mobilities depending on the presence or absence of Ca^{2+}. A comparative SDS-PAGE analysis of all novel mutants with the wildtype is shown in Fig. 2. All proteins showed a lower mobility in the absence of Ca^{2+} indicating that the conformation of the corresponding Ca^{2+}-free GCAP1 form was less compact than the Ca^{2+}-loaded form. Furthermore, this experiment demonstrated that the mutant GCAP1 forms can undergo a Ca^{2+}-induced conformational change similar as the wildtype.

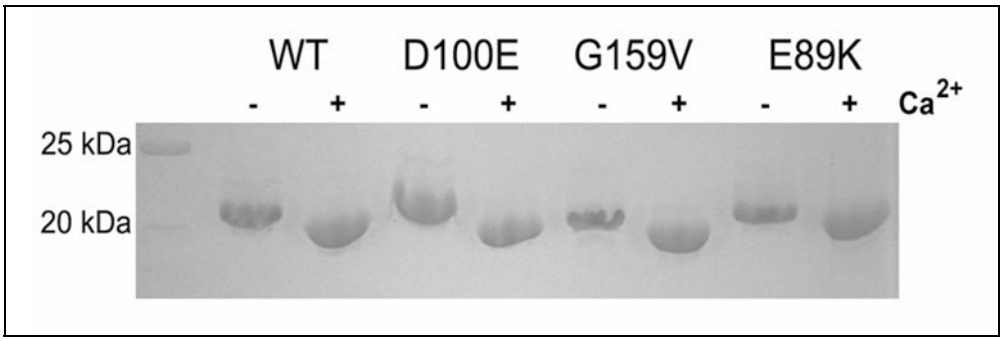

Figure 2. Ca^{2+}-dependent electrophoretic mobility shift of wildtype and mutants of GCAP1. In all cases the myristoylated proteins were analysed by SDS-PAGE in the presence of 2 mM $CaCl_2$ (+) or EGTA (-) in a 12% polyacrylamide gel; wildtype GCAP1 (WT), p.Asp100Glu (D100E), p.Gly159Val (G159V) and p.Glu89Lys (E89K). Molecular mass standards are seen on the left side.

Trp fluorescence

In a second approach we investigated the Ca^{2+}-triggered conformational changes by measuring changes in Trp fluorescence. It is well established for wildtype GCAP1 that Ca^{2+}-induced changes in Trp fluorescence exhibit a biphasic pattern in the absence of $Mg^{2+}$and a loss of phase I in the presence of Mg^{2+} (Peshenko and Dizhoor, 2006). While this biphasic pattern with a minimum of fluorescence intensity around 1 µM Ca^{2+} was also observed for wildtype GCAP1 in the absence of Mg^{2+} (Fig. 3), no phase II was seen for all studied GCAP1 mutants as shown in Fig 3 A-C. However, in the presence of Mg^{2+} the mutant p.Asp100Glu showed a similar profile of fluorescence intensity like the wildtype as there was no prominent increase below 1 µM Ca^{2+} (loss of phase I), but a prominent increase above 1µM (phase II). Similar results were obtained with all other mutants (data not shown). In conclusion, wildtype and mutants of GCAP1 underwent very similar Ca^{2+}-induced conformational changes in the presence of Mg^{2+}, but removing Mg^{2+} revealed a significant difference between wildtype and mutants in the exposure of Trp residues (see discussion for more details).

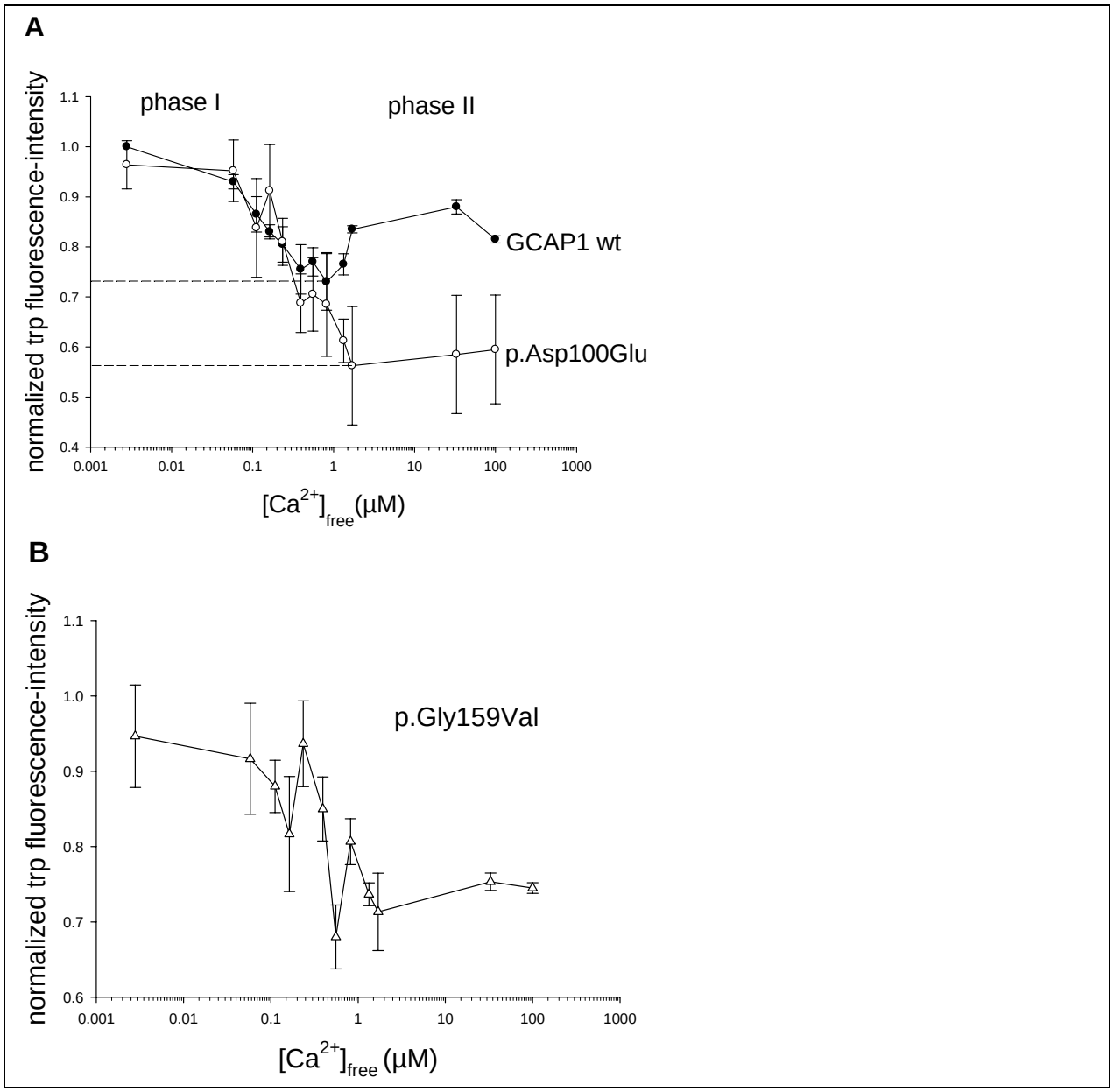

Figure 3. Tryptophane fluorescence emission as a function of the free Ca^{2+} concentration for wildtype and GCAP1 mutants. Relative fluorescence emission of intrinsic Trp fluorescence was measured at 336 nm (excitation at 280 nm) and normalized to the maximal value. (A) Wildtype (•) and p.Asp100Glu (°) GCAP1 were present at a concentration of 1.5 µM. Recordings were performed in the absence of $MgCl_2$ at different free Ca^{2+} concentration as indicated. Phase I and II are indicated with the dashed lines pointing to the minimum around 1 µM Ca^{2+}. The same protocol of recording Trp fluorescence and evaluation of the data was performed with p.Gly159Val (B) and p.Glu89Lys.

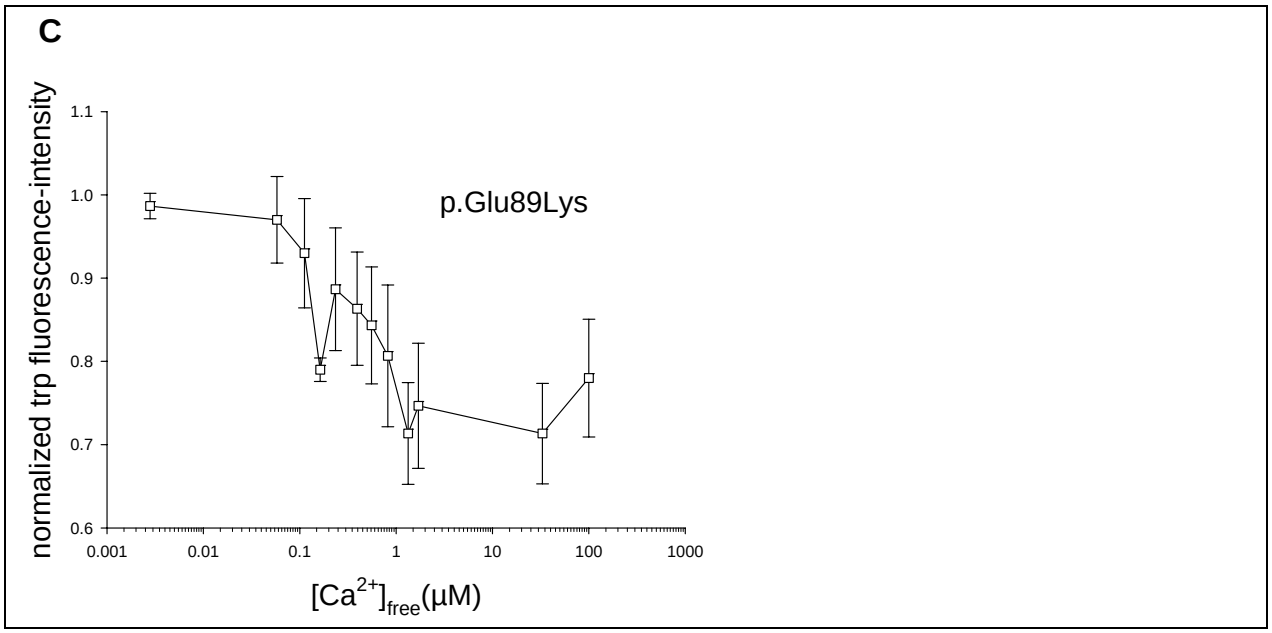

Figure 3. Tryptophane fluorescence emission as a function of the free Ca^{2+} concentration for wildtype and GCAP1 mutants. Relative fluorescence emission of intrinsic Trp fluorescence was measured at 336 nm (excitation at 280 nm) and normalized to the maximal value. (C). Data are the mean ± s.d. of 3 result sets.

GCAP1-dependent regulation of guanylate cyclase activity

We determined the GCAP1-dependent regulation of GC activity using an in vitro approach. Maximal GC activities at low Ca^{2+} concentration (in the presence of EGTA) were at 17-24 nmol cGMP per min and mg rhodopsin for the wildtype and the mutants p.Asp100Glu and p.Gly159Val (Table 2). Only the mutant p.Glu89Lys showed a lower maximal activity (~ 10 nmol per min and mg rhodopsin), but the difference to wildtype GCAP1 was not statistically significant (t-test $P \geq 0.05$).

In order to determine the apparent affinity of GCAP1 forms for its target we determined the GC activity at increasing GCAP1 concentrations yielding the EC_{50} values, i.e. the concentration at which the GC activity is halfmaximal. For all GCAP1 mutants EC_{50} values were nearly identical (Table 2) indicating that control of GC activity by the mutant GCAPs was performed with similar affinities for the target.

Table 2. Regulation of ROS-GC1 by wildtype and mutants of GCAP1.

GCAP1-form	activity at high [Ca^{2+}]	activity at low [Ca^{2+}]	x-fold activation	EC_{50} (µM)	IC_{50} (µM)
bGCAP1 wt	0.24 +/- 0.04	16.9 +/- 4.0	41.2	1.37 +/- 0.17	0.78 +/- 0.20
p.Asp100Glu	0.67 +/- 0.36	23.7 +/- 0.67	35.4	1.27 +/- 0.15	21.94 +/- 1.3
p.Gly159Val	0.4 +/- 0.34	21.07 +/- 5.1	52.7	1.33 +/- 0.12	14.45 +/- 1.98
p.Glu89Lys	0.61 +/- 0.09	10.5 +/- 2.44	17.2	1.36 +/- 0.02	4.67 +/- 0.4

Guanylate cyclase activity is expressed as nmol cGMP produced per min and per mg of rhodopsin. EC_{50} and IC_{50} values correspond to protein (GCAP1) and Ca^{2+} concentration. The ratio of activity at low to high Ca^{2+} concentration is expressed as x-fold activation.

We further analyzed the Ca^{2+}-dependent activation profiles of all mutants by measuring the GC activities as a function of free Ca^{2+} in the presence of saturating wildtype and mutant GCAP1 concentrations thereby determining the IC_{50} values for each form, i.e. the Ca^{2+} concentration at which the GC activity is halfmaximal. All novel mutants exhibited a shift of their IC_{50} values to higher free Ca^{2+} and could be ranked in the following

order: p.Asp100Glu > p.Gly159Val > p.Glu89Lys (Table 2 and 3). The most dramatic shift was observed with p.Asp100Glu (Fig. 4), where the change of the IC_{50} value was ~28-fold. For p.Gly159Val a 18-fold shift was observed and for p.Glu89Lys a six-fold shift of the IC_{50}.

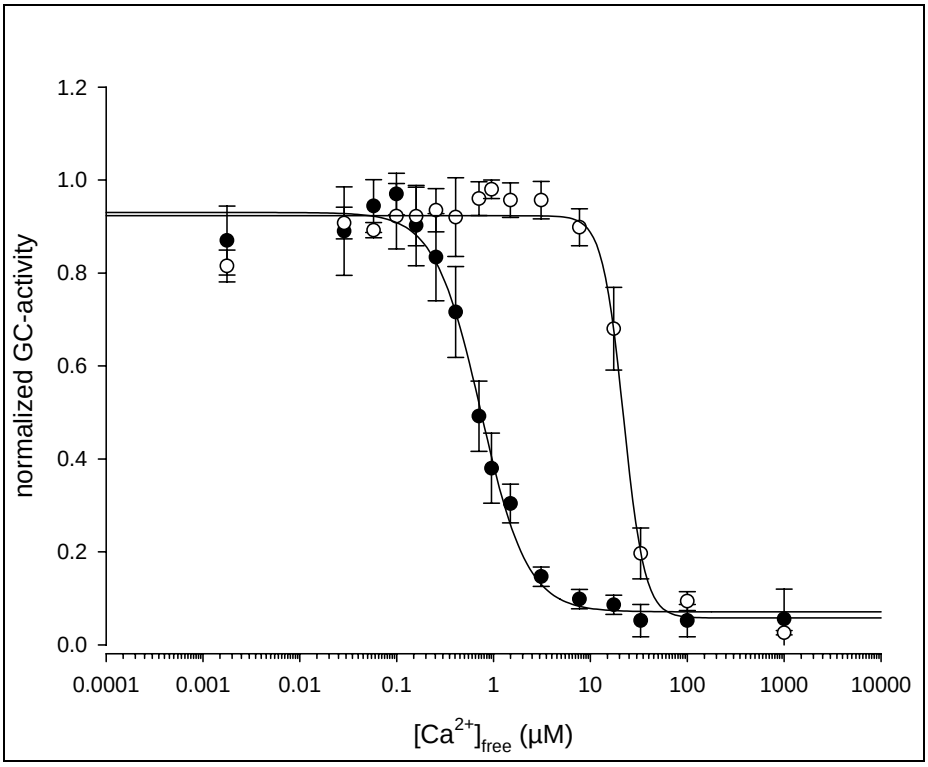

Figure 4. Regulation of ROS-GC1 by wildtype and p.Asp100Glu GCAP1. Washed bovine ROS membranes containing ROS-GC1 were reconstituted with 10 µM wildtype (•) and p.Asp100Glu (O) GCAP1 at varying Ca^{2+} concentration. Guanylate cyclase activity was measured as nmol cGMP/min/mg rhodopsin and is expressed as normalized activity.

Thus, our results indicate that these GCAP1 mutants were able to activate ROS-GC1 at higher Ca^{2+} concentrations than the wildtype, while at the same time the affinity for the target enzyme appeared unaffected. Therefore, the impairment caused by the mutations leads to a specific gain of function that results in a cone dystrophy.

DISCUSSION

Here we report the identification of three novel and one previously reported *GUCA1A* gene mutations causing adCD and adCRD and present a detailed functional and molecular characterization of the mutant proteins with a focus on their Ca^{2+}-sensing and guanylate cyclase regulating properties.

GCAPs are neuronal calcium sensor (NCS) proteins with four EF-hand Ca^{2+}-binding sites (EF1-EF4), but only EF-hands 2,3 and 4 are capable of binding Ca^{2+}-ions, whereas EF-hand 1 is not functional at physiological concentrations of Ca^{2+}. GCAPs operate as Ca^{2+}-sensors and respond to a change of intracellular Ca^{2+} concentrations with a change of their conformation. The switch between the Ca^{2+}-free and Ca^{2+}-bound state of GCAPs is the essential trigger for regulating the target enzyme, the photoreceptor guanylate cyclase ROS-GC1. So far, several mutations in GCAP1 were discovered in patients suffering from retinal diseases, but only one case involving a GCAP2 mutation was reported (Sato, et al., 2005). The GCAP1 mutations, investigated here occur within highly conserved regions in EF-hand 3 and EF-hand 4. Thus, several molecular consequences of these

mutations are conceivable and our study has addressed the critical steps in GCAP1 signaling. These steps include Ca^{2+}-induced conformational changes, the interaction with the target, ROS-GC1 and the Ca^{2+}-sensitivity of GC regulation. For a comprehensive summary of our results see Table 3.

Table 3. Biochemical and functional properties of wildtype and mutants of GCAP1.

Property		**bGCAP1 wt**	**p.Asp100Glu**	**p.Gly159Val**	**p.Glu89Lys**
Gelshift at saturating [Ca^{2+}]		+	+	+	+
GC-activation		+	+	+	+
IC_{50} difference from WT		1	28	18	6
Trp-fluorescence	Phase I	+	+	+	+
	Phase II	+	-	-	-

All mutants in this study showed an electrophoretic mobility shift, when Ca^{2+} was complexed by EGTA during electrophoresis indicating no principle impairment of conformational changes. Our Trp fluorescence analysis showed that the conformational change at Ca^{2+} concentration above 1 µM observed with the wildtype in the absence of Mg^{2+} was different in all tested mutants, because there was no phase II. Changes in Trp fluorescence above 1 µM Ca^{2+} (phase II) were reported to correlate with Trp at position 94 moving into a more hydrophobic environment (Peshenko and Dizhoor, 2006). From the lack of phase II we conclude that Trp94 does not move into a more apolar environment in GCAP1 mutants. From the position of Trp94 in the incoming helix of EF-hand 3 we suggest that the Ca^{2+}-binding to EF-hand 3 and/ or EF-hand 4 is altered. Interestingly, this observation was only made in the absence of Mg^{2+}. Addition of Mg^{2+} seems to compensate for any conformational disturbances seen in the mutants.

The concentration at which mutant and wildtype GCAP1 activate ROS-GC1 (EC_{50}) was very similar for all tested proteins and showed that they interact with similar apparent affinities. In addition, this result provides an independent proof that our heterologously expressed and purified proteins work properly and are not misfolded due to the cell extraction and purification procedures.

Although the GCAP1 mutants were in principle able to activate ROS-GC1, they did this with significant differences in their Ca^{2+}-sensitivities. The largest shift in the IC_{50} value was observed with the mutant p.Asp100Glu that harbours an amino acid exchange in the loop region of EF hand 3. This position assigned as 1(+X) is invariant in all known EF-hand motifs so far (Gifford, et al., 2007). Exchange of Asp for Glu adds only a CH_2-group to the side chain, but with dramatic consequences for the coordination of Ca^{2+}. The 28-fold shift in Ca^{2+}-sensitivity to higher free Ca^{2+} concentration revealed that this mutant was not fully Ca^{2+}-loaded under conditions where wildtype GCAP1 would be saturated with Ca^{2+}. The point mutation probably alters significantly the complexing properties of EF-hand 3 leading to a loop with lower affinity for Ca^{2+}. This lower affinity could for example result from an increase in the dissociation rate. The other two mutations were located in either the incoming helix of EF-hand 3 (p.Glu89Lys) or the outgoing helix of EF-hand 4 (p.Gly159Val). Both mutations shifted the IC_{50} to higher free [Ca^{2+}] but to a lesser degree. Since the amino acid exchange occurred at a position that is not directly involved in complexing Ca^{2+} the shift might originate from a distortion of the helices making the overall coordination of Ca^{2+} to EF-hand 3 or 4 less favourable.

A cone cell expressing one of the mutated GCAPs described in this study would be transformed in a state of nearly permanent synthesis of cGMP, because the normal dark level of Ca^{2+} would be insufficient to suppress ROS-GC1 activity. The mutants p.Asp100Glu and p.Gly159Val would activate ROS-GC1 at micromolar Ca^{2+} concentrations that are far above the cellular dark concentration (s. IC_{50}-values in Table 2). But even the five-fold shift of Ca^{2+}-sensitivity of the p.Glu89Lys mutant would significantly disturb the balance of cGMP synthesis and hydrolysis. The permanently elevated synthesis of cGMP would keep a larger fraction of the cyclic nucleotide-gated channels open. Affected photoreceptor cells would need more photons than unaffected cells to activate the cGMP hydrolyzing cascade in order to close the channels. This increase in the flux of cGMP, normally observed in the presence of background light (Nikonov, et al., 2000), would already occur under dark conditions and would shift the light sensitivity of the photoreceptor.

Further, any mutation that leads to a change in cGMP homeostasis would in turn also affect the Ca^{2+}-homeostasis in photoreceptor cells as these two messengers are strongly coupled via feedback mechanisms. These effects would lead to a further disregulation of phototransduction involving other Ca^{2+}-binding proteins.

Incomplete suppression of GC activity at high Ca^{2+} concentration was also observed with other GCAP1 mutants (p.Tyr99Cys, p.Asn104Lys, p.Ile143AsnThr, p.Leu151Phe, and p.Glu155Gly, Dizhoor, et al., 1998; Sokal, et al., 1998; Jiang, et al., 2008; Nishiguchi, et al., 2004; Sokal, et al., 2005; Wilkie, et al., 2001) pointing to the importance of an exactly balanced cGMP synthesis for undisturbed vision.

Mutations in GUCA1A were identified in 4 of 24 unrelated patients accounting for 17% of adCD and adCRD in this study. Most patients with GUCA1A mutations suffered from adCD. Within families a clear progression with age was observed (family ZD1 and ZD172). In the oldest patient in our series who experienced a disease duration of more than sixty years a conversion from a pure cone to a cone rod dystrophy was seen (ZD172 16033/M). Although the identified GCAP1 mutations show different functional properties as described above, they basically all affect cGMP and calcium homeostasis more or less dramatically and thus might clinically converge on one common phenotype: a slowly progressing cone photoreceptor dysfunction, as GCAP1 is predominantly expressed in cones. Studies on transgenic mice also revealed the importance of GCAP1 in cone vision, since it can restore the recovery of cone responses in the absence of GCAP2 (Pennesi, et al., 2003). Rod photoreceptors eventually become also affected in cone dystrophies. However, defects in GCAP1 signaling might partially be compensated by the presence of almost equimolar amounts of GCAP2 in mammalian rods (Hwang, et al., 2003), which could explain why rod dysfunction is sometimes delayed for several years.

REFERENCES

Bradford MM. 1976. A rapid and sensitive method for the quantitation of microgram quantities of protein utilizing the principle of protein-dye binding. Anal Biochem. 72**:** 248–254.

Cuenca N, Lopez S, Howes K, Kolb H. 1998. The localization of guanylyl cyclase-activating proteins in the mammalian retina. Invest Ophthalmol Vis Sci 39:1243-1250.

Dizhoor AM, Boikov SG, Olshevskaya EV. 1998. Constitutive activation of photoreceptor guanylate cyclase by Y99C mutant of GCAP-1. J Biol Chem 273:17311-17314.

Downes S, Holder G, Fitzke F, Payne A, Warren M, Bhattacharya S, Bird A. 2001. Autosomal Dominant Cone and Cone-Rod Dystrophy With Mutations in the Guanylate Cyclase Activator 1A Gene-Encoding Guanylate Cyclase Activating Protein-1. Arch Ophthalmol 119:96-105.

Frins S, Bönigk W, Müller F, Kellner R, Koch KW. 1996. Functional characterization of a guanylyl cyclase-activating protein from vertebrate rods. Cloning, heterologous expression, and localization. J Biol Chem 271:8022–8027.

Gifford JL, Walsh, MP, Vogel, HJ. 2007. Structures and metal-ion-binding properties of the Ca2+-binding helix-loop-helix EF-hand motifs. Biochem J. 405: 199-221.

Haeseleer F, Sokal I, Li N, Pettenati M, Rao N, Bronson D, Wechter R, Baehr W, Palczewski K. 1999. Molecular Characterization of a Third Member of the Guanylyl Cyclase-activating Protein Subfamily. J Biol Chem 274:6526-6535.

Hamel C. 2007. Cone rod dystrophies. Orphanet J Rare Dis 2:7.

Helten A, Säftel W, Koch, KW. 2007. Expression level and activity profile of membrane bound guanylate cyclase type 2 in rod outer segments. J Neurochem 103:1439-1446.

Hwang JY, Koch KW. 2002a. Calcium and myristoyl-dependent properties of guanylate cyclase-activating protein-1 and protein-2. Biochemistry 41:13021-13028.

Hwang JY, Koch KW. (2002b). The myristoylation of the neuronal Ca^{2+}-sensors guanylate cyclase-activating protein 1 and 2. Biochim Biophys Acta 1600:111-117.

Hwang JY, Lange C, Helten A, Höppner-Heitmann D, Duda T, Sharma RK, Koch KW. 2003. Regulatory modes of rod outer segment membrane guanylate cyclase differ in catalytic efficiency and Ca^{2+}-sensitivity. Eur J Biochem 270:3814-3821.

Jiang L, Katz B, Yang Z, Zhao Y, Faulkner N, Hu J, Baird J, Baehr W, Creel D, Zhang K. 2005. Autosomal dominant cone dystrophy caused by a novel mutation in the GCAP1 gene (GUCA1A). Mol Vis 11:143-151.

Jiang L, Wheaton D, Bereta G, Zhang K, Palczewski K, Birch D, Baehr W. 2008. A novel GCAP1(N104K) mutation in EF-hand 3 (EF3) linked to autosomal dominant cone dystrophy. Vision Res 48: 2425-2432.

Koch KW; Helten A. 2008. Guanylate cyclase-based signaling in photoreceptors and retina in Signal Transduction in the Retina (Fliesler, S.J. and Kisselev, O.G., Eds.) Taylor and Francis CRC Press. Chapter 6:121–143.

Laemmli UK. 1970. Cleavage of structural proteins during assembly of the head of bacteriophage T4. Nature 227:680-685.

Marmor M, Holder G, Seeliger M, Yamamoto S, and. 2004. Standard for clinical electroretinography (2004 update). Doc Ophthalmol 108(2):107-114.

Mendez A, Burns M, Sokal I, Dizhoor A, Baehr W, Palczewski K, Baylor D, Chen J. 2001. Role of guanylate cyclase-activating proteins (GCAPs) in setting the flash sensitivity of rod photoreceptors. Proc Natl Acad Sci 98:9948-9953.

Merin S. 2005. Inherited Eye Diseases: Diagnosis and Management: Taylor & Francis.

Michaelides M, Hardcastle A, Hunt D, Moore A. 2006. Progressive cone and cone-rod dystrophies: phenotypes and underlying molecular genetic basis. Survey of Ophthalmology 51:232-258.

Michaelides M, Wilkie SE, Jenkins S, Holder GE, Hunt DM, Moore AT, Webster AR. 2005. Mutation in the gene GUCA1A, encoding guanylate cyclase-activating protein 1, causes cone, cone-rod, and macular dystrophy. Ophthalmology 112:1442-1447.

Newbold RJ, Deery EC, Walker CE, Wilkie SE, Srinivasan N, Hunt DM, Bhattacharya SS, Warren MJ. 2001 The destabilization of human GCAP1 by proline to leucine mutation might cause cone-rod dystrophy. Hum Mol Genet 10: 47-54.

Nikonov S, Lamb TD, Pugh EN Jr. 2000 The role of steady phosphodiesterase activity in the kinetics and sensitivity of the light-adapted salmander rod photoresponse. J Gen Physiol 116:795-824.

Nishiguchi K, Sokal I, Yang L, Roychowdhury N, Palczewski K, Berson E, Dryja T, Baehr W. 2004. A novel mutation (I143NT) in guanylate cyclase-activating protein 1 (GCAP1) associated with autosomal dominant cone degeneration. Invest Ophthalmol Vis Sci 45:3863-3870.

Olshevskaya EV, Calvert PD, Woodruff ML, Peshenko IV, Savchenko AB, Makino CL, Ho YS, Fain GL, Dizhoor AM. 2004. The Y99C mutation in guanylyl cyclase-activating protein 1 increases intracellular Ca2+ and causes photoreceptor degeneration in transgenic mice. J Neurosci 24:6078-6085.

Palczewski K, Subbaraya I, Gorczyca WA, Helekar BS, Ruiz CC, Ohguro H, Huang J, Zhao X, Crabb JW, Johnson RS, Walsh KA, Gray-Keller MP, Detwiler PB, Baehr W. 1994. Molecular cloning and characterization of retinal photoreceptor guanylyl cyclase-activating protein. Neuron 13**:**395–404.

Payne A, Downes S, Bessant D, Taylor R, Holder G, Warren M, Bird A, Bhattacharya S. 1998. A mutation in guanylate cyclase activator 1A (GUCA1A) in an autosomal dominant cone dystrophy pedigree mapping to a new locus on chromosome 6p21.1. Hum Mol Genet 7:273.

Pennesi M, Howes K, Baehr W, Wu S. 2003. Guanylate cyclase-activating protein (GCAP) 1 rescues cone recovery kinetics in GCAP1/GCAP2 knockout mice. Proc Natl Acad Sci 100:6783-6788.

Peshenko IV, Dizhoor AM. 2006. Ca^{2+} and Mg^{2+} binding properties of GCAP-1. Evidence that Mg^{2+}-bound form is the physiological activator of photoreceptor guanylyl cyclase. J Biol Chem 281**:**23830–23841.

Sato M,Nakazawa M, Usui T, Tanimoto N, Abe H, Ohguro H. 2005. Mutations in the gene coding for guanylate cyclase-activating protein 2 (GUCA1B gene) in patients with autosomal dominant retinal dystrophies. Graefe´s Arch Clin Exp Ophthalmol 243:235-242.

Sokal I, Li N, Surgucheva I, Warren MJ, Payne AM, Bhattacharya SS, Baehr W, Palczewski K. 1998. GCAP1 (Y99C) mutant is constitutively active in autosomal dominant cone dystrophy. Mol Cell 2:129-133.

Sokal I, Dupps W, Grassi M, Brown JJ, Affatigato L, Roychowdhury N, Yang L, Filipek S, Palczewski K, Stone E and others. 2005. A novel GCAP1 missense mutation (L151F) in a large family with autosomal dominant cone-rod dystrophy (adCORD). Invest Ophthalmol Vis Sci 46:1124-1132.

Stephen R, Palczewski K, Sousa MC. 2006. The crystal structure of GCAP3 suggests molecular mechanism of GCAP-linked cone dystrophies. J Mol Biol 359:266-275.

Thompson JD, Higgins DG, Gibson TJ. 1994. CLUSTAL W: improving the sensitivity of progressive multiple sequence alignment through sequence weighting, position-specific gap penalties and weight matrix choice. Nucleic Acids Res 22:4673-4680.

Wildeman W, van Ophuizen E, den Dunnen JT, Taschner PE. 2008. Improving sequence variant descriptions in mutation databases and literature using the Mutalyzer sequence variation nomenclature checker. Hum Mutat 29: 6-13.

Wilkie SE, Li Y, Deery EC, Newbold RJ, Garibaldi D, Bateman JB, Zhang H, Lin W, Zack DJ, Bhattacharya SS and others. 2001. Identification and functional consequences of a new mutation (E155G) in the gene for GCAP1 that causes autosomal dominant cone dystrophy. Am J Hum Genet 69:471-480.